

Reprogramming human A375 amelanotic melanoma cells by catalase overexpression: Reversion or promotion of malignancy by inducing melanogenesis or metastasis

Candelaria Bracalente^{1,2}, Noelia Salguero¹, Cintia Notcovich¹, Carolina B. Müller³, Leonardo L. da Motta³, Fabio Klamt³, Irene L. Ibañez^{1,2}, Hebe Durán^{1,2,4}

¹Departamento de Micro y Nanotecnología, Comisión Nacional de Energía Atómica, San Martín, Buenos Aires, B1650KNA, Argentina

²Consejo Nacional de Investigaciones Científicas y Tecnológicas, Buenos Aires, C1033AAJ, Argentina

³Laboratório de Bioquímica Celular, Departamento de Bioquímica, Instituto de Ciências Básicas da Saúde, Universidade Federal do Rio Grande do Sul, Porto Alegre, 90035 003, Brasil

⁴Escuela de Ciencia y Tecnología, Universidad Nacional de San Martín, San Martín, Buenos Aires, B1650HMP, Argentina

Correspondence to: Hebe Durán, **email:** hduran@cnea.gov.ar

Keywords: melanoma, catalase, ROS, melanogenesis and metastasis

Received: October 27, 2015

Accepted: March 28, 2016

Published: May 07, 2016

ABSTRACT

Advanced melanoma is the most aggressive form of skin cancer. It is highly metastatic and dysfunctional in melanogenesis; two processes that are induced by H₂O₂. This work presents a melanoma cell model with low levels of H₂O₂ induced by catalase overexpression to study differentiation/dedifferentiation processes. Three clones (A7, C10 and G10) of human A375 amelanotic melanoma cells with quite distinct phenotypes were obtained. These clones faced H₂O₂ scavenging by two main strategies. One developed by clone G10 where ROS increased. This resulted in G10 migration and metastasis associated with the increased of cofilin-1 and CAP1. The other strategy was observed in clone A7 and C10, where ROS levels were maintained reversing malignant features. Particularly, C10 was not tumorigenic, while A7 reversed the amelanotic phenotype by increasing melanin content and melanocytic differentiation markers. These clones allowed the study of potential differentiation and migration markers and its association with ROS levels *in vitro* and *in vivo*, providing a new melanoma model with different degree of malignancy.

INTRODUCTION

Melanoma arises from malignant transformation of melanocytes. Besides, it is highly metastatic and among the most resistant cancers to treatments [1]. Loss of pigmentation in melanoma is common in advanced lesions because of dysfunction in melanogenesis proteins. Tyrosinase (TYR) and the tyrosinase related proteins 1 and 2 (TYRP1 and TYRP2 respectively), are the main proteins involved in melanogenesis [2].

Melanoma cells produce high amounts of reactive oxygen species (ROS) compared with their non-tumoral counterpart [3, 4]. ROS participate in tumor development by inducing oncogenic mutation and signal transduction pathways associated with cell proliferation [5, 6], differentiation [7] and the pro-invasive metastatic program

[7–12]. Antioxidant enzymes, such as superoxide dismutase (SOD), catalase, peroxidases and peroxiredoxins, control the levels of ROS. H₂O₂ increases in a wide variety of malignant cells through an imbalance in the antioxidant system (AOS), characterized by high levels of SOD and low levels of H₂O₂ detoxifying enzymes, as catalase [4, 13, 14]. Indeed, tumor cell proliferation is inhibited by decreasing H₂O₂ through catalase.

Catalase is the main enzyme that dissipates the H₂O₂ produced during melanin synthesis [15]. There is a correlation among catalase activity, melanin content and TYR activity [15, 16]. Therefore, considering that H₂O₂ inhibits TYR, TYRP1 and TYRP2 [17], the high levels of H₂O₂ associated with low catalase activity in melanoma [18–20] would be relevant in the induction of the amelanotic phenotype.

Cell invasion and migration are critical for metastasis and indicate poor prognosis. To migrate, cancer cells develop invadopodia through actin polymerization/depolymerization cycles [21–23]. Metastatic cells present high levels of cofilin-1, a key regulator of actin polymerization. Cofilin-1 severs actin filaments, favoring actin polymerization and so migration [24, 25]. Overexpression of cofilin-1 was associated with loss of cell polarity in colon adenocarcinoma cells [26] and has been used as poor prognosis marker related to metastasis in lung cancer patients [27, 28]. Adenylyl cyclase-associated protein 1 (CAP1) facilitates actin and cofilin-1 recycling, essential for cell migration [29, 30]. CAP1 overexpression was associated with migration in pancreatic cancer cells [31]. However, the behavior of these proteins in melanoma has received little attention.

In this study, a differential compensation to H₂O₂ scavenging by catalase overexpression in A375 amelanotic melanoma cells was demonstrated. Cells responded to H₂O₂ scavenging by two main strategies: increasing ROS, which resulted in metastasis or maintaining ROS levels, reversing malignant features. Therefore, to overcome the inhibition of cell proliferation induced by catalase overexpression, cells changed the redox status leading to distinct phenotypes ranging from reversion to promotion of melanoma malignancy. Finally, this model allowed the evaluation *in vitro* and *in vivo* of migration related proteins and melanocytic differentiation markers and their association with oxidative stress levels.

RESULTS

Characterization of melanoma cells overexpressing catalase

Catalase overexpression on human amelanotic melanoma A375 cells gave rise to three clones: A375-A7 (A7), A375-C10 (C10) and A375-G10 (G10). A375 and A375 cells transfected with the empty vector (PCDNA3) were used as control. An increase in catalase activity and expression was observed for all clones vs PCDNA3 ($p < 0.05$) (Figure 1A–1C). H₂O₂ levels decreased in all clones when compared to control ($p < 0.05$), with the unexpected increase in G10 ROS production ($p < 0.05$) (Figure 1D–1F). No changes were found neither in glutathione peroxidase activity nor in peroxiredoxin 2 expression (Supplementary Figure S1). These results indicate that catalase overexpression dissipates H₂O₂ in all clones and only G10 induced a redox response that increased its basal ROS levels.

Stable expression of catalase down-regulated cell proliferation parameters

Cell proliferation, anchorage-independent cell growth and ERK activity decreased in all clones vs control ($p < 0.05$). AKT activity was significantly lower only for

A7 (Figure 2A–2D). Together, these results confirm that catalase overexpression decreases H₂O₂, inhibiting cell proliferation parameters. In view of the similar results between PCDNA3 and A375 cells, most *in vitro* assays were performed using only PCDNA3 as control.

Different cell polarity degree was induced by catalase overexpression

Cell polarity, particularly melanoma cell dendricity is associated with more differentiated phenotype while its disruption is a hallmark of cancer [32–35]. Increased polarity was found in A7 vs control ($p < 0.05$). On the contrary, a dramatic loss of polarity was observed in G10 vs control ($p < 0.001$). An increase of multipolar cells in A7 and apolar cells in G10 was observed vs control (< 0.01) (Figure 2E–2F). This indicates higher cell differentiation degree in A7, as it resembles melanocytes dendritic like-structure [34–36]. Conversely, the apolar feature of G10 may be associated to amoeboid migration, one of the two main categories of cell movement, characteristic of rounded or ellipsoid cells [25, 37, 38]. To confirm these ideas, melanocyte differentiation features and cell migration parameters were evaluated.

Catalase overexpression increased melanocyte differentiation

Melanogenesis parameters were evaluated to verify whether the multipolarity found in A7 implies its evolution to a normal melanocyte. Results showed an increase in melanin content, TYR activity and TYRP1 expression in A7 compared with the amelanotic control ($p < 0.05$). Moreover, A7 increased the ability to proliferate after UV-A irradiation compared with control ($p < 0.01$) (Figure 3A–3D). Given that melanin protects melanocytes from UV radiation, these results indicate that A7 evolved to a melanotic and differentiated phenotype.

Catalase overexpression induced melanoma cell migration

In order to evaluate if G10 had developed the ability to migrate, wound healing (Figure 4A and 4B) and transwell assay (Figure 4C) were performed. Increased migration was observed in G10 vs control and the other clones ($p < 0.05$) (Figure 4A–4C). Note that cells were not synchronized in terms of cell proliferation for wound healing. Therefore, considering that G10 as the other two clones are less proliferative, its increased migration could not be accounted for differences in proliferation rate.

Actin polymerization state, cofilin-1 and CAP1 were evaluated because of their relevance in cell migration. Increased actin fibers (F-actin) and F-actin aggregates in the leading edge of G10 cells were observed (Figure 5A). Furthermore, cofilin-1 and CAP1 expression increased in

G10 vs control ($p < 0.05$) (Figure 5A–5D). CAP1 was differentially located in protrusions of G10 cells with fiber actin (Supplementary Figure S2). These results indicate an increased actin polymerization state in G10 that favors its ability to migrate.

Differential tumorigenicity was induced by catalase overexpression

Regarding tumorigenesis, A7 induced pigmented tumors denoting increased differentiation, although they grew similar to controls (A375 and PCDNA3). On the contrary, tumors from G10 had more than 40 days delay in growth with significant decrease in size when compared to controls, even allowing to grow the same time since they appear, consistent with it less *in vitro* proliferation rate. C10 never induced tumors, even after 6 month since inoculation. No differences were found between controls (Figure 6A–6B).

Representative images of H&E stained tumor tissue sections are shown (Supplementary Figure S3). High cell proliferation can be observed in tumors induced by controls and A7, but A7 tumors present areas with brownish granules of melanin deposits (Supplementary

Figure S3), supporting the *in vitro* results of melanin synthesis and differentiation. On the other hand, G10 tumors were mostly necrotic. Note that as C10 did not induce tumors, no H&E/immunohistochemistry was performed.

Besides, an increased expression of TYRP1 in A7 ($p < 0.05$) and of cofilin-1 and CAP1 in G10 compared with controls were found ($p < 0.05$) (Figure 6C–6D). These results confirmed *in vivo* that stable overexpression of catalase induced either melanogenesis or migration, which could be associated with the unchanged levels of ROS in A7 or its increased levels in G10.

Considering the migration ability of G10, *in vivo* assay of tumor metastasis was performed. Pulmonary metastatic nodules were induced only by G10, indicating its evolution to a more aggressive phenotype (Figure 6E) and reinforcing the idea that its increased ROS levels could be associated with its malignant phenotype.

DISCUSSION

This work shows that overexpression of catalase in A375 melanoma cells inhibits proliferation in agreement with previous results [4, 39]. Besides, anchorage-

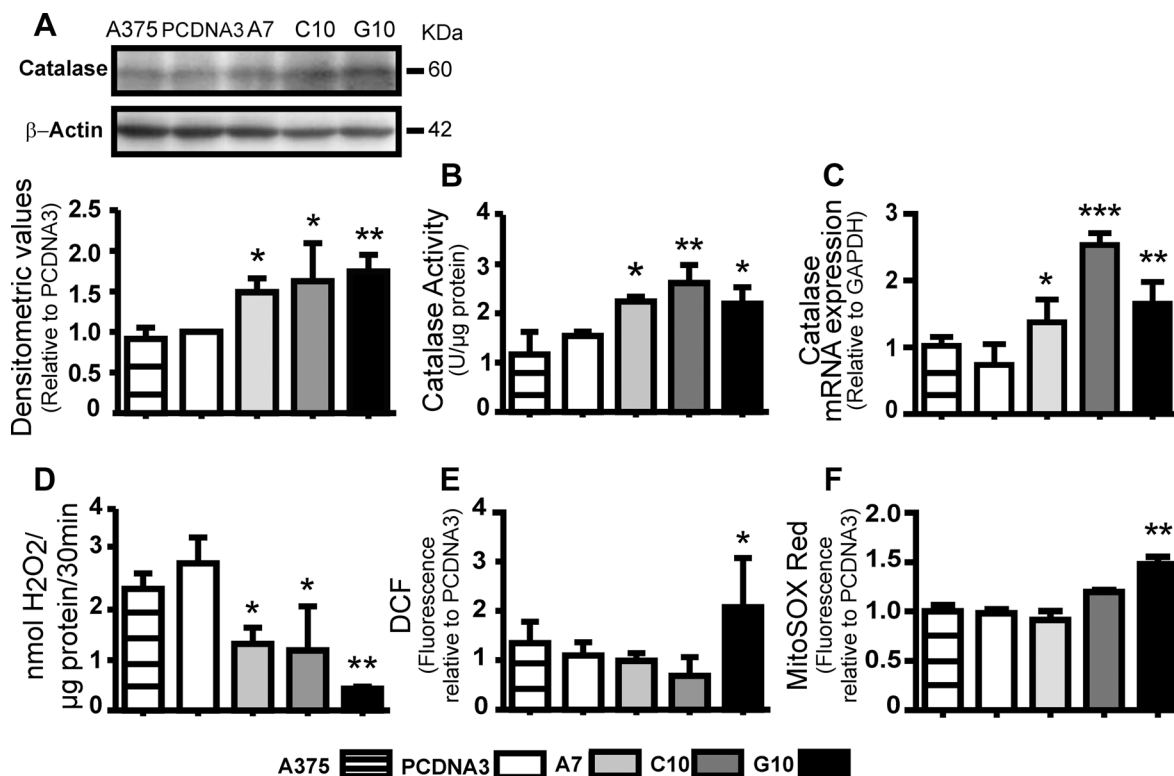


Figure 1: Catalase-transfected A375 cells (A7, C10 and G10) decreased H₂O₂ levels but differentially induced ROS levels. Control: A375 cells transfected with empty vector (PCDNA3) and not transfected (A375). (A) Representative immunoblot images of catalase and β -actin with its densitometric analysis. Actin values were used to normalize samples. Full length blots are included as Supplementary Figure S4. (B) Determination of catalase activity by spectrophotometric method. (C) Catalase mRNA expression by qPCR (D) Quantification of H₂O₂ production by Amplex[®] Red kit. (E–F) Intracellular ROS levels by quantification of DCF and MitoSOX Red mean fluorescence. Data are expressed as mean \pm SD. * $p < 0.05$; ** $p < 0.01$; *** $p < 0.001$ vs control (PCDNA3).

independent cell growth inhibition was also found. However, the response to catalase overexpression led to quite distinct phenotypes that ranged from reversion to promotion of malignancy. When cells responded to H_2O_2 decrease increasing ROS levels, migration and metastasis were induced (G10), but when ROS levels did not change, less aggressive (A7) or nonmalignant (C10) phenotypes were generated.

Tumors progress with continuous ROS increase due to an AOS imbalance, which is characterized by low levels of catalase and glutathione peroxidase [4, 13, 39, 40]. Given that glutathione peroxidase activity and peroxiredoxin 2 expression did not change in these clones, H_2O_2 levels mainly decreased by the overexpression of catalase.

Besides, ERK1/2 activation increases proliferation [41]. Hydrogen peroxide can increase ERK1/2 activity by the oxidation of its phosphatases [42, 43]. These studies could explain how the decrease of H_2O_2 in these clones reduced its ERK1/2 activity together with cell proliferation and anchorage-independent cell growth.

Dedifferentiation/differentiation are associated with more or less aggressive tumors [32, 33]. Clone A7 enhanced polarity with melanoma cell dendricity, a parameter of melanoma differentiation [34, 35]. Moreover, the activation of melanogenic pathway was observed in A7 by the increase in melanin content, tyrosinase activity and TYRP1 expression. The increase of catalase activity correlates with melanin content [16]. Pigmentation and melanocyte differentiation markers

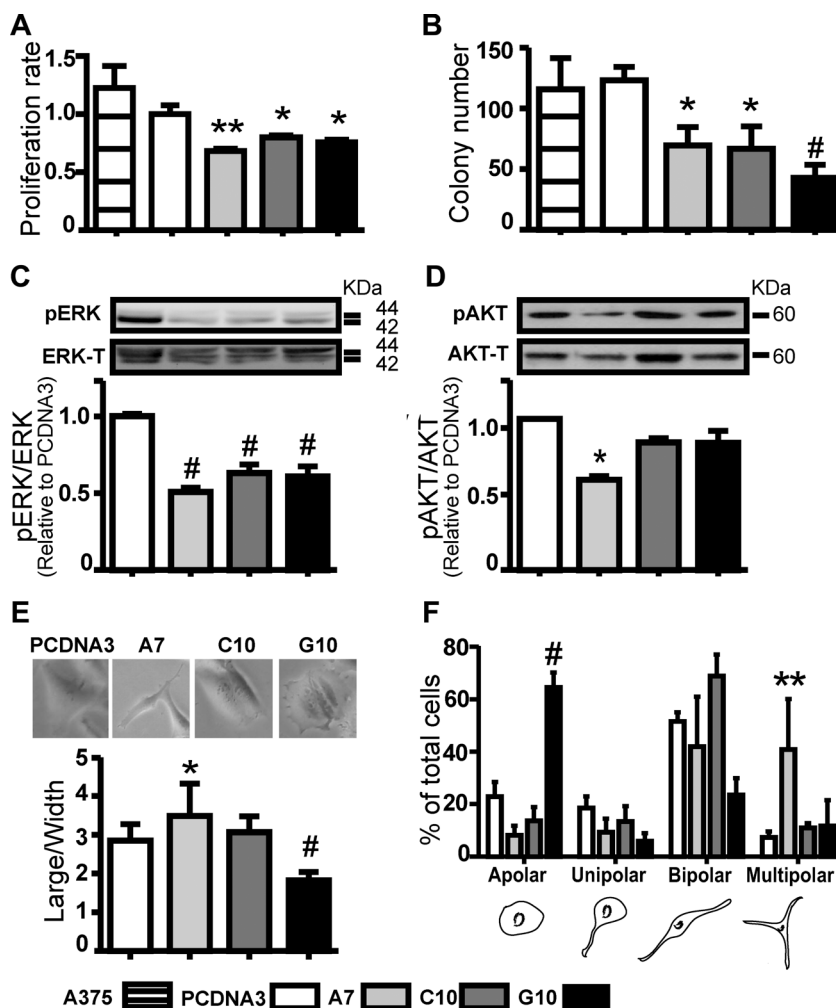


Figure 2: Catalase overexpression down-regulated melanoma cell proliferation parameters and induced different cell polarity degree. A375 cells transfected with catalase (A7, C10 and G10) or not transfected (A375) relative to control, A375 cells transfected with empty vector (PCDNA3). (A) Cell proliferation rate evaluated by MTT assay. (B) Anchorage independent cell growth by soft agar assay. Results represent average number of colony per field, as described in supplementary material. (C–D) Representative immunoblot images of pERK, pAkt, total ERK and Akt. Full length blots are included as Supplementary Figure S4. Densitometric values of pERK or pAkt relative to total ERK or Akt respectively are shown. (E) Large to width cell ratio quantification. (F) Cell polarity degree was scored as shown in the cartoon below and presented as percentage of total cells scored. Cell scored/condition: 150. Data are expressed as mean \pm SD. * $p < 0.05$; ** $p < 0.01$; # $p < 0.001$ vs control.

(tyrosinase and TYRP1) decreased by high H₂O₂ levels [15, 17]. Furthermore, tyrosinase and TYRP1 correlates inversely with tumor stage and its progression to the amelanotic phenotype [44–46]. Supporting the increased UV-A tolerance of A7, melanocytes offset deleterious effects of UV radiation by melanin and catalase [15, 47]. Therefore, these previous reports support how A7 turned to a differentiated and therefore less aggressive phenotype.

Only A7 showed a significant decrease of Akt activity. In this regard, inhibition of Akt in melanoma cells increases melanogenesis pathway, by inducing MITF, meanwhile the inhibition of ERK did not [48, 49]. These previous studies could explain why melanogenesis was induced in A7 but not in C10 and G10. Thus, the induction

of differentiation in A7 by catalase overexpression could be mediated by the inhibition of Akt activation, reinforcing its participation in the melanogenesis pathway.

Clone G10 showed a clear change towards dedifferentiation, revealed by the loss of polarity, characteristic of migration and metastasis progression [25, 38]. The fact that G10 increased ROS levels, although decreased H₂O₂, suggest that other ROS are responsible for the oxidative status of G10. The expression of proteins related to migration and metastasis induced by ROS [10] can explain the ability of G10 to migrate and metastasize. Therefore, switching to a migrating phenotype could be “an escape program” from high ROS levels [10]. In a mouse melanoma model, the antioxidant N-acetylcysteine

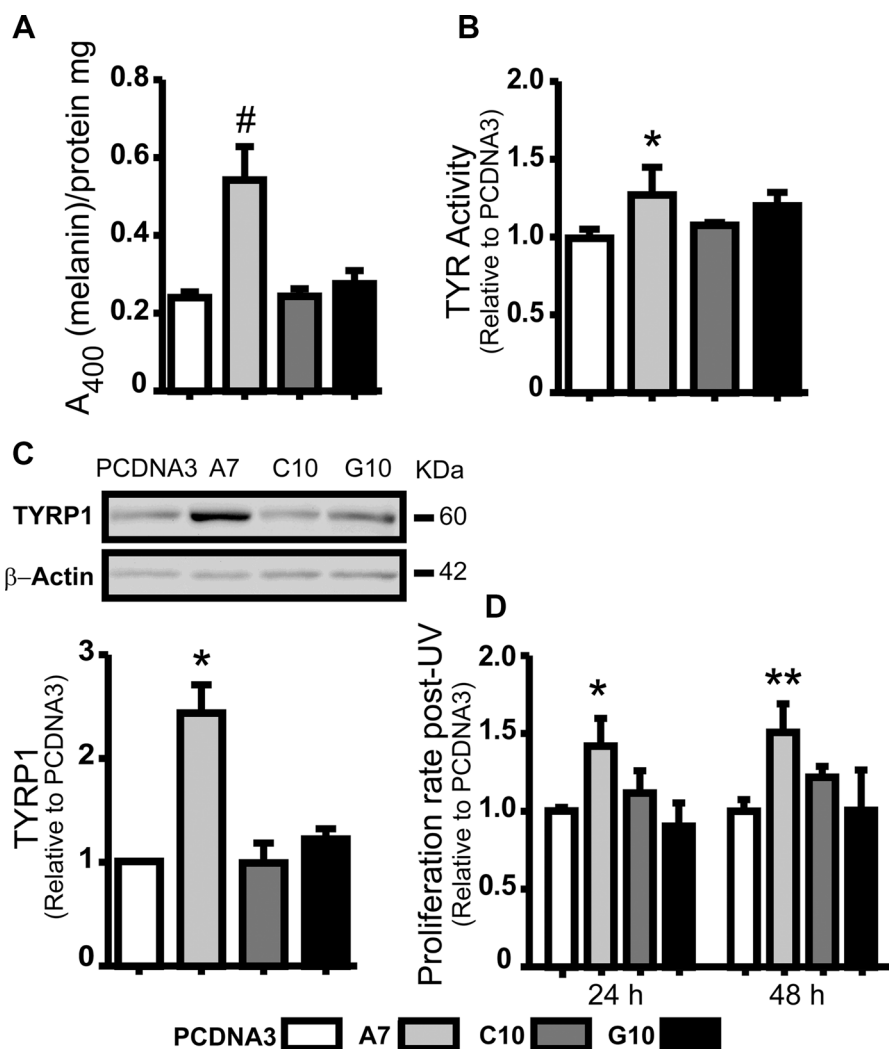


Figure 3: Catalase overexpression induced melanoma cell differentiation. A375 cells transfected with catalase (A7, C10 and G10) relative to control, A375 cells transfected with empty vector (PCDNA3). (A) Melanin content determination in cell lysates by absorbance at 400 nm. Protein quantification was used to standardize cell samples. (B) TYR activity was evaluated indirectly by L-DOPA oxidase activity assay. Dopachrome levels were determined at 492 nm. (C) Representative immunoblot images of TYRP1 and β-actin protein expressions with its densitometric analysis. Actin densitometric values were used to normalize samples. Full length blots are included as Supplementary Figure S5. (D) Cell proliferation rate 24 and 48 hours post-UV radiation evaluated by MTT assay. Data are expressed as mean ± SD. **p* < 0.05; ***p* < 0.01; #*p* < 0.001 vs control.

(NAC) increased lymph node metastases but had no impact on the number and size of primary tumors [50]. These results agree with the metastatic ability and the small primary tumor size of G10.

Melanoma cells invade and metastasize by amoeboid or mesenchymal migration [37, 38, 51]. Amoeboid migration, characteristic of round cells, is induced by actin-rich filopodia at the leading edge of cells facilitating protrusions [24, 37], as observed in G10. Increase of cofilin-1 and CAP1 was found in G10. These proteins favors actin polymerization and so migration [29]. Cofilin-1 is a key factor in tumor cell migration and metastasis, being overexpressed in a wide variety of cancers [24, 26, 27, 52]. Cofilin-1 is activated by dephosphorylation through the phosphatase Slingshot-1L (SSH-1L) [53, 54]. High levels of ROS activate cofilin-1 through the release of SSH-1L from its regulatory protein when oxidized by ROS, increasing cell migration [55]. Thus, high ROS production found in G10 could activate cofilin-1 by dephosphorylation. Colocalization of CAP1 with F-actin in the leading edge of cells has been involved in metastasis. Moreover, repression of

cofilin-1 or CAP1 in metastatic cells inhibited migration [25, 31, 56, 57]. Therefore, not only the high levels of CAP1 and cofilin-1, but also the high ROS production found in G10 could be key events that promote migration and metastasis.

In vivo assays validated *in vitro* results. Tumorigenicity was completely inhibited in C10 and decreased in G10, consistent with the inhibition of proliferation and the antitumor effect of catalase [14, 58]. Even though A7 was tumorigenic, tumors were pigmented with increased expression of TYRP1. This confirms that A7 is a differentiated melanoma, which could be associated with a less aggressive phenotype. On the contrary, the increase of cofilin-1 and CAP1 together with the metastasis induced by G10 *in vivo* supports the fact that G10 evolved to an aggressive phenotype.

In conclusion, these cells faced H₂O₂ dissipation by two main strategies: maintaining or increasing ROS levels. Malignant features were reversed by catalase overexpression when ROS levels remained unchanged as demonstrated in C10 and A7. Moreover, when H₂O₂ scavenging was associated to Akt inactivation,

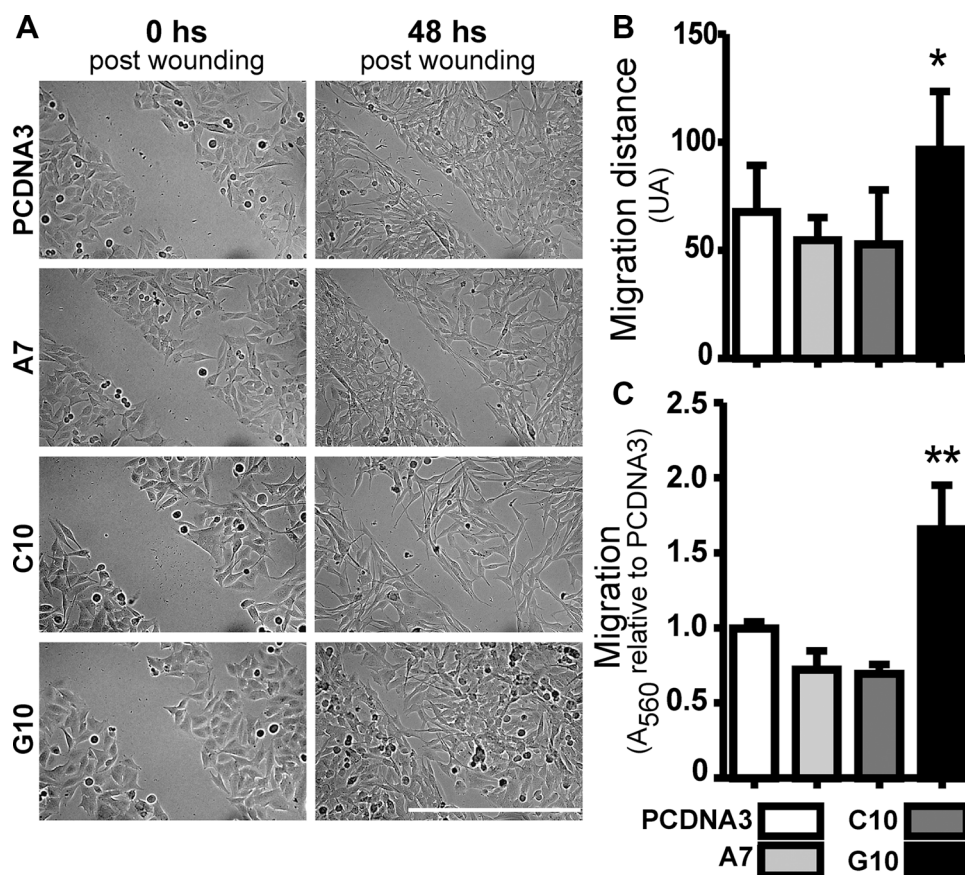


Figure 4: Catalase overexpression induced melanoma cell migration. A375 cells transfected with catalase (A7, C10 and G10) relative to control, A375 cells transfected with empty vector (PCDNA3). (A) Representative images of wound-healing assay, 0 and 48 hours post-wounding. Bar represents 200 μ m. (B) Quantification of migration distance calculated as the average difference between the distance in arbitrary units (AU) at time 0 and 48 hours after wounding. (C) Evaluation of migration capacity by trans-well assay. Absorbance at 560 nm indicates the amount of cells passing through membrane pores. Data are expressed as mean \pm SD. * $p < 0.05$; ** $p < 0.01$ vs control.

melanogenesis pathway was triggered, as shown in A7 where TYRP1, tyrosinase and melanin content increased. On the other hand, when the response to catalase overexpression led to high ROS levels, amoeboid migration and actin polymerization were induced by both increasing cofilin-1 and CAP1 proteins, which are the driving force of migration and metastasis, as demonstrated in G10.

The oxidative stress conditions that exist within the tumor and its microenvironment exert strong adaptive pressure on cancer cells, which in order to survive, promote the expression of ROS pathways reprogramming the transcriptome, proteome and metabolism [59]. Considering that H₂O₂ scavenging inhibits cell proliferation, we propose herein that melanoma cells triggered different responses

to reach a redox homeostasis overcoming the effects on survival induced by catalase. Consistent with these idea, gene expression microarrays analysis of A7 and G10 [60] confirmed both *in vitro* and *in vivo* results and revealed coexpressed AOS genes upregulated in A7 and downregulated in G10, which could explain the different redox responses generated by each clone. Thus, even though it must be necessary to ascertain the results presented here in other cellular models, it is noteworthy that overexpression of an antioxidant enzyme, such as catalase, could favor not only the reversion of malignant processes but also the progression to a worse outcome. Therefore, taking into account that antioxidants can both, prevent or promote

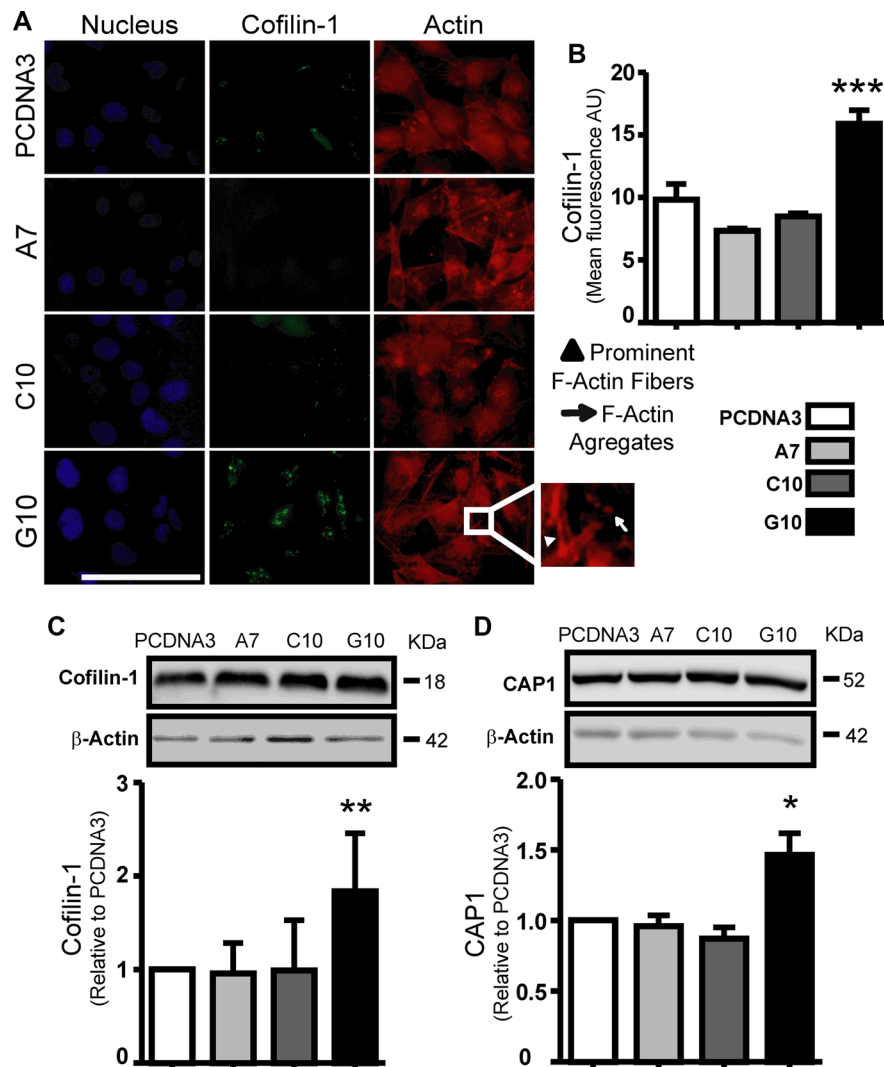


Figure 5: Catalase overexpression induced cofilin-1 and CAP1 expression. A375 cells transfected with catalase (A7, C10 and G10) relative to control, A375 cells transfected with empty vector (PCDNA3). (A) Representative immunocytofluorescence images of cofilin-1 with their corresponding actin and nuclear staining using rhodamine phalloidin and DAPI respectively. Bar represents 100 μ m. Inset image of G10 exhibits its prominent F-actin and F-actin aggregates. (B) Quantification of cofilin-1 expression as the mean cell fluorescence arbitrary units (AU). (C–D) Representative immunoblot images of cofilin-1 and CAP1 protein expression with their respective densitometric analysis. Actin values were used to normalize samples. Full length blots are included as Supplementary Figure S5. Data are expressed as mean \pm SD. * p < 0.05; ** p < 0.01; *** p < 0.001 vs control.

cancer progression [50, 61–63], it is necessary to reconsider the use of antioxidants as a strategy against cancer without studying compensatory responses of the AOS.

In addition, the development of these stable clones with distinct characteristics in terms of antioxidant metabolism, pigmentation, migration and metastasis

provides a new melanoma model for studying mechanisms associated with differentiation/dedifferentiation and malignant progression under the same genetic background. Finally, this work allowed proposing TYRP1, cofilin-1 and CAP1 as potential markers to detect melanomas with varying degrees of aggressiveness.

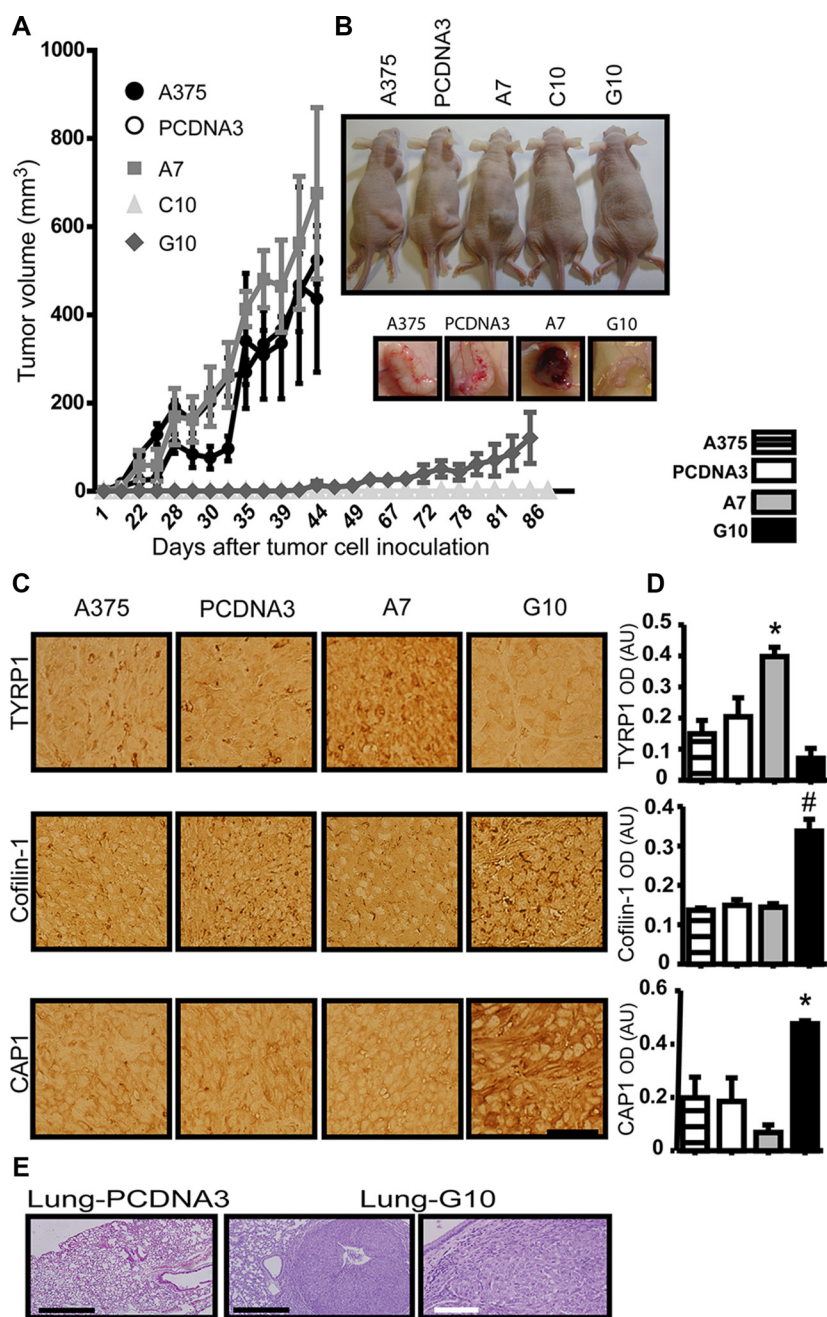


Figure 6: *In vivo* validation of *in vitro* results in tumors induced by melanoma cells overexpressing catalase. Nude mice inoculated with A375 cells transfected with catalase (A7, C10 and G10), with empty vector (PCDNA3) or not transfected (A375). (A) Tumor growth curves over time post-inoculation by monitoring tumor volume throughout time. (B) Representative images of mice inoculated with each cell type and the respective tumors of the tumorigenic ones: A375, PCDNA3, A7 and G10. (C) Representative images of TYRP1, cofilin-1 and CAP1 IHC detection in tissue sections of tumors induced by A375, PCDNA3, A7 and G10 cells. Bar represents 50 μ m. (D) Quantification of IHC by optic densitometric (OD) analysis of images. Data are expressed as mean \pm SD. * p < 0.05; # p < 0.001 vs control (PCDNA3). (E) Lung tissue sections stained with H&E. Representative images of G10 lung nodules indicate its metastatic ability. Control lung tissue section is also shown. Black bars represent 500 μ m and white bar 100 μ m.

MATERIALS AND METHODS

Cell culture and catalase overexpression melanoma model

Low-passages human amelanotic melanoma cell line A375 was kindly donated by Dr. E. Medrano (Huffington Center on Aging, Departments of Molecular & Cellular Biology and Dermatology, Baylor College of Medicine, Houston, Texas, USA). All the experiments with these cells were performed with less than 5 passages from thawing. Cells were cultured as previously described [4]. Stable transfected cells were maintained in identical conditions with 700 $\mu\text{g/ml}$ geneticin (Sigma). Cells were regularly tested to be mycoplasma-free.

A375 cells were transfected with pcDNA3 vector harboring the human catalase cDNA (p-CAT) using Lipofectamine 2000 (Invitrogen) [4]. Stable transfectants were selected in medium with 1500 $\mu\text{g/ml}$ geneticin. Three resistant clones A375-A7, A375-C10 and A375-G10, referred in this work as A7, C10 and G10 respectively, were obtained by clonal dilution. Given that catalase inhibits cell proliferation only three clones were possible to obtain. Transfected cells with empty vector were used as negative control and named A375-PCDNA3, referred here as PCDNA3.

In vitro experiments

Determination of catalase and redox parameters

Catalase mRNA expression was determined by quantitative real-time PCR (qPCR). Forward and reverse primer sequences were: 5'cctttctgtgaagatgcgcg3 and 5'ggcggtagtgatgcaggatag'3 respectively. Cycling conditions are detailed in Supplementary Table S1. For protein expression western blot was performed using anti-catalase antibody (Calbiochem, EMD Milipore) and the detection of β -actin (Sigma antibody) as loading control. Catalase activity was measured using a spectrophotometric assay [4].

The intracellular levels of H_2O_2 were evaluated by spectrophotometry according to Amplex[®] Red kit (Invitrogen). A standard curve of H_2O_2 was performed. Results were expressed as H_2O_2 nmol released in 30 min per protein μg .

The levels of ROS were determined by 2',7'-dichlorodihydro-fluorescein diacetate (DCFH-DA, Sigma) assay [64] and MitoSOX[™] Red (Invitrogen) [65].

Glutathione peroxidase (GPx) activity was measured by an indirect spectrophotometric assay [66, 67]. Peroxiredoxin 2 expression was detected by western blot using anti-peroxiredoxin 2 (Sigma) and β -actin antibody (Sigma) as loading control.

Determination of cell proliferation parameters

Proliferation was determined by MTT assay [68]. Anchorage independent cell growth was evaluated by soft agar colony formation assay.

The levels of the active form of ERK1/2 and Akt (p-ERK1/2 and p-Akt) related to the total form of these proteins were detected by western blot as a measure of their activity.

Cell polarity

Cell polarity was evaluated by measuring the cell length/width ratio (L/W) and cells were classified as apolar, unipolar, bipolar or multipolar as shown in Figure 2F [25].

Determination of melanogenesis parameters

Melanin content was evaluated in cell lysates by spectrophotometry at 400 nm and expressed per protein mg. Tyrosinase activity was assayed by measuring the L-3, 4-dihydroxyphenylalanine (L-DOPA) oxidase activity. The dopachrome levels were determined at 492 nm [69]. TYRP1 expression was assessed by western blot using anti-TYRP1 antibody (Abcam) and β -actin antibody (Sigma) as loading control.

Cell response to UV-A radiation

After 24 hours culture, 5000 cells were irradiated with 29 kJ/m^2 total irradiation dose [70].

Cell proliferation was evaluated 24 and 48 hours post irradiation through MTT assay.

Cell migration: Wound healing and transwell assay

A scratch in the cell monolayer was performed and migration extent was evaluated at 48 hours after healing. Transwell migration assay was performed using the CytoSelect[™] Cell Migration Assay Kit, according to manufacturer's indications (Cell Biolabs, Inc).

Evaluation of cofilin-1, CAP1 and actin polymerization state

Standard immunocytofluorescence and western blot using anti-cofilin-1 or anti-CAP1 antibodies (Abcam) were performed. Detection of β -actin (Sigma antibody) was used as loading control in western blot. Rhodamine-phalloidin (Sigma) staining was used for actin visualization.

In vivo experiments

Six-week-old female athymic nude (nu/nu) mice were obtained from the CNEA animal facility (Argentina). Animals were kept under conventional housing conditions. To evaluate the *in vivo* effect by catalase overexpression, tumors and metastasis were induced by injecting 2.5×10^6 cells subcutaneously in one flank or through the tail vein respectively, using 5 animals per experimental condition. As control of cell viability of tail vein inoculated cells at the moment of injection, cells were inoculated subcutaneously in 2 nude mice per condition. All procedures were carried out according to the Laboratory Animal Care and Use guidelines from CNEA and to the relevant international guidelines.

Evaluation of tumor growth and metastasis

Tumor growth was evaluated by determining tumor volume every other day during up to 3 month. To study the development of metastasis, mice autopsy was conducted. Tumors and organs with naked eyes metastasis were processed for histopathological examination (H&E) and immunohistochemistry.

Immunohistochemistry detection of TYRP1, cofilin-1 and CAP1

Standard immunohistochemistry was performed using proper antibodies and Super Sensitive IHC Detection Systems (BioGenex) or Picture-MAX Polymer (Invitrogen) kits following manufacturer's instructions. Rabbit anti-TYRP1, cofilin-1 and CAP1 antibodies (Abcam) were used.

Statistical analysis

Significant differences between group means were assessed by one-way analysis of variance followed by Dunn's multiple comparisons test. For tumor growth analysis, when parametric tests were not possible to apply, Friedman test for matched observations was performed followed by Dunnett's multiple comparisons test. *P*-values lower than 0.05 were considered significant for all tests.

Detailed description of all methods is included in Supplementary Materials.

ACKNOWLEDGMENTS AND FUNDING

The authors thank to the members of Departamento de Radiobiología, Comisión Nacional de Energía Atómica, for their valuable assistance and continuous support.

CONFLICTS OF INTEREST

None declared.

GRANT SUPPORT

Agencia Nacional de Promoción Científica y Tecnológica, Argentina (PICT 2007-01628); MCTI /CNPQ/CBAB Cooperação Internacional em Biotecnologia (465113/2014-1); Departamento de Micro y Nanotecnología, Comisión Nacional de Energía Atómica, Argentina; Fundación Florencio Fiorini, Argentina.

REFERENCES

1. Zhang G, Li G. Novel multiple markers to distinguish melanoma from dysplastic nevi. *PLoS One*. 2012; 7: e45037.
2. Schiaffino MV. Signaling pathways in melanosome biogenesis and pathology. *Int J Biochem Cell Biol*. 2010; 42:1094–1104.
3. Picardo M, Grammatico P, Roccella F, Roccella M, Grandinetti M, Del Porto G, Passi S. Imbalance in the antioxidant pool in melanoma cells and normal melanocytes from patients with melanoma. *J Invest Dermatol*. 1996; 107:322–326.
4. Ibanez IL, Bracalente C, Notcovich C, Tropper I, Molinari BL, Policastro LL, Duran H. Phosphorylation and subcellular localization of p27Kip1 regulated by hydrogen peroxide modulation in cancer cells. *PLoS ONE*. 2012; 7: e44502.
5. Cakir Y, Ballinger SW. Reactive species-mediated regulation of cell signaling and the cell cycle: the role of MAPK. *Antioxid Redox Signal*. 2005; 7:726–740.
6. Arnold RS, Shi J, Murad E, Whalen AM, Sun CQ, Polavarapu R, Parthasarathy S, Petros JA, Lambeth JD. Hydrogen peroxide mediates the cell growth and transformation caused by the mitogenic oxidase Nox1. *Proc Natl Acad Sci U S A*. 2001; 98:5550–5555.
7. Meyskens FL, Jr., Farmer P, Fruehauf JP. Redox regulation in human melanocytes and melanoma. *Pigment Cell Res*. 2001; 14:148–154.
8. Condeelis J, Singer RH, Segall JE. The great escape: when cancer cells hijack the genes for chemotaxis and motility. *Annu Rev Cell Dev Biol*. 2005; 21:695–718.
9. Nishikawa M. Reactive oxygen species in tumor metastasis. *Cancer Lett*. 2008; 266:53–59.
10. Pani G, Galeotti T, Chiarugi P. Metastasis: cancer cell's escape from oxidative stress. *Cancer Metastasis Rev*. 2010; 29:351–378.
11. Behrend L, Henderson G, Zwacka RM. Reactive oxygen species in oncogenic transformation. *Biochem Soc Trans*. 2003; 31:1441–1444.
12. Zhang Y, Du Y, Le W, Wang K, Kieffer N, Zhang J. Redox control of the survival of healthy and diseased cells. *Antioxid Redox Signal*. 2011; 15:2867–2908.
13. Policastro L, Molinari B, Larcher F, Blanco P, Podhajcer OL, Costa CS, Rojas P, Duran H. Imbalance of antioxidant enzymes in tumor cells and inhibition of proliferation and malignant features by scavenging hydrogen peroxide. *Mol Carcinog*. 2004; 39:103–113.
14. Hyoudou K, Nishikawa M, Ikemura M, Kobayashi Y, Mendelsohn A, Miyazaki N, Tabata Y, Yamashita F, Hashida M. Prevention of pulmonary metastasis from subcutaneous tumors by binary system-based sustained delivery of catalase. *J Control Release*. 2009; 137: 110–115.
15. Maresca V, Flori E, Briganti S, Mastrofrancesco A, Fabbri C, Mileo AM, Paggi MG, Picardo M. Correlation between melanogenic and catalase activity in *in vitro* human melanocytes: a synergic strategy against oxidative stress. *Pigment Cell Melanoma Res*. 2008; 21:200–205.
16. Schallreuter KU, Salem MM, Hasse S, Rokos H. The redox—biochemistry of human hair pigmentation. *Pigment Cell Melanoma Res*. 2011; 24:51–62.

17. Jimenez-Cervantes C, Martinez-Esparza M, Perez C, Daum N, Solano F, Garcia-Borron JC. Inhibition of melanogenesis in response to oxidative stress: transient downregulation of melanocyte differentiation markers and possible involvement of microphthalmia transcription factor. *J Cell Sci.* 2001; 114:2335–2344.
18. Szatrowski TP, Nathan CF. Production of large amounts of hydrogen peroxide by human tumor cells. *Cancer Res.* 1991; 51:794–798.
19. Policastro LL, Ibanez IL, Duran HA, Soria G, Gottifredi V, Podhajcer OL. Suppression of cancer growth by nonviral gene therapy based on a novel reactive oxygen species-responsive promoter. *Mol Ther.* 2009; 17:1355–1364.
20. Picardo M, Maresca V, Eibenschutz L, De Bernardo C, Rinaldi R, Grammatico P. Correlation between antioxidants and phototypes in melanocytes cultures. A possible link of physiologic and pathologic relevance. *J Invest Dermatol.* 1999; 113:424–425.
21. Bravo-Cordero JJ, Hodgson L, Condeelis J. Directed cell invasion and migration during metastasis. *Curr Opin Cell Biol.* 2012; 24:277–283.
22. Wang W, Goswami S, Lapidus K, Wells AL, Wyckoff JB, Sahai E, Singer RH, Segall JE, Condeelis JS. Identification and testing of a gene expression signature of invasive carcinoma cells within primary mammary tumors. *Cancer Res.* 2004; 64:8585–8594.
23. Olson MF, Sahai E. The actin cytoskeleton in cancer cell motility. *Clin Exp Metastasis.* 2009; 26:273–287.
24. Wang W, Eddy R, Condeelis J. The cofilin pathway in breast cancer invasion and metastasis. *Nat Rev Cancer.* 2007; 7:429–440.
25. Sidani M, Wessels D, Mouneimne G, Ghosh M, Goswami S, Sarmiento C, Wang W, Kuhl S, El-Sibai M, Backer JM, Eddy R, Soll D, Condeelis J. Cofilin determines the migration behavior and turning frequency of metastatic cancer cells. *J Cell Biol.* 2007; 179:777–791.
26. Popow-Wozniak A, Mazur AJ, Mannherz HG, Malicka-Blaszkiewicz M, Nowak D. Cofilin overexpression affects actin cytoskeleton organization and migration of human colon adenocarcinoma cells. *Histochem Cell Biol.* 2012; 138:725–736.
27. Muller CB, de Barros RL, Castro MA, Lopes FM, Meurer RT, Roehe A, Mazzini G, Ulbrich-Kulczynski JM, Dal-Pizzol F, Fernandes MC, Moreira JC, Xavier LL, Klamt F. Validation of cofilin-1 as a biomarker in non-small cell lung cancer: application of quantitative method in a retrospective cohort. *J Cancer Res Clin Oncol.* 2011; 137:1309–1316.
28. Castro MA, Dal-Pizzol F, Zdanov S, Soares M, Muller CB, Lopes FM, Zanotto-Filho A, da Cruz Fernandes M, Moreira JC, Shacter E, Klamt F. CFL1 expression levels as a prognostic and drug resistance marker in nonsmall cell lung cancer. *Cancer.* 2010; 116:3645–3655.
29. Moriyama K, Yahara I. Human CAP1 is a key factor in the recycling of cofilin and actin for rapid actin turnover. *J Cell Sci.* 2002; 115:1591–1601.
30. Hubberstey AV, Mottillo EP. Cyclase-associated proteins: CAPacity for linking signal transduction and actin polymerization. *FASEB J.* 2002; 16:487–499.
31. Yamazaki K, Takamura M, Masugi Y, Mori T, Du W, Hibi T, Hiraoka N, Ohta T, Ohki M, Hirohashi S, Sakamoto M. Adenylate cyclase-associated protein 1 overexpressed in pancreatic cancers is involved in cancer cell motility. *Lab Invest.* 2009; 89:425–432.
32. Lee M, Vasioukhin V. Cell polarity and cancer—cell and tissue polarity as a non-canonical tumor suppressor. *J Cell Sci.* 2008; 121:1141–1150.
33. Royer C, Lu X. Epithelial cell polarity: a major gatekeeper against cancer? *Cell Death Differ.* 2011; 18:1470–1477.
34. Saez-Ayala M, Montenegro MF, Sanchez-Del-Campo L, Fernandez-Perez MP, Chazarra S, Freter R, Middleton M, Pinero-Madrona A, Cabezas-Herrera J, Goding CR, Rodriguez-Lopez JN. Directed phenotype switching as an effective antimelanoma strategy. *Cancer Cell.* 2013; 24:105–119.
35. Serafino A, Sinibaldi-Vallebona P, Lazzarino G, Tavazzi B, Rasi G, Pierimarchi P, Andreola F, Moroni G, Galvano G, Galvano F, Garaci E. Differentiation of human melanoma cells induced by cyanidin-3-O-beta-glucopyranoside. *FASEB J.* 2004; 18:1940–1942.
36. Zhao Y, Liu J, McMartin KE. Inhibition of NADPH oxidase activity promotes differentiation of B16 melanoma cells. *Oncol Rep.* 2008; 19:1225–1230.
37. Wolf K, Mazo I, Leung H, Engelke K, von Andrian UH, Deryugina EI, Strongin AY, Bocker EB, Friedl P. Compensation mechanism in tumor cell migration: mesenchymal-amoeboid transition after blocking of pericellular proteolysis. *J Cell Biol.* 2003; 160:267–277.
38. Friedl P, Wolf K. Plasticity of cell migration: a multiscale tuning model. *J Cell Biol.* 2010; 188:11–19.
39. Glorieux C, Dejeans N, Sid B, Beck R, Calderon PB, Verrax J. Catalase overexpression in mammary cancer cells leads to a less aggressive phenotype and an altered response to chemotherapy. *Biochem Pharmacol.* 2011; 82:1384–1390.
40. Gupta A, Butts B, Kwei KA, Dvorakova K, Stratton SP, Briehl MM, Bowden GT. Attenuation of catalase activity in the malignant phenotype plays a functional role in an *in vitro* model for tumor progression. *Cancer Lett.* 2001; 173:115–125.
41. Berger MF, Garraway LA. Applications of genomics in melanoma oncogene discovery. *Hematol Oncol Clin North Am.* 2009; 23:397–414, vii.
42. Traore K, Sharma R, Thimmulappa RK, Watson WH, Biswal S, Trush MA. Redox-regulation of Erk1/2-directed phosphatase by reactive oxygen species: role in signaling TPA-induced growth arrest in ML-1 cells. *J Cell Physiol.* 2008; 216:276–285.

43. Jimenez LA, Zanella C, Fung H, Janssen YM, Vacek P, Charland C, Goldberg J, Mossman BT. Role of extracellular signal-regulated protein kinases in apoptosis by asbestos and H₂O₂. *Am J Physiol*. 1997; 273: L1029–1035.
44. Ghanem G, Fabrice J. Tyrosinase related protein 1 (TYRP1/gp75) in human cutaneous melanoma. *Mol Oncol*. 2011; 5:150–155.
45. Bolander A, Agnarsdottir M, Stromberg S, Ponten F, Hesselius P, Uhlen M, Bergqvist M. The protein expression of TRP-1 and galectin-1 in cutaneous malignant melanomas. *Cancer Genomics Proteomics*. 2008; 5:293–300.
46. Orlow SJ, Silvers WK, Zhou BK, Mintz B. Comparative decreases in tyrosinase, TRP-1, TRP-2, and Pmel 17/silver antigenic proteins from melanotic to amelanotic stages of syngeneic mouse cutaneous melanomas and metastases. *Cancer Res*. 1998; 58:1521–1523.
47. Meredith P, Sarna T. The physical and chemical properties of eumelanin. *Pigment Cell Res*. 2006; 19:572–594.
48. Zhang W, Tsan R, Nam DH, Lu W, Fidler IJ. Loss of adhesion in the circulation converts amelanotic metastatic melanoma cells to melanotic by inhibition of AKT. *Neoplasia*. 2006; 8:543–550.
49. Shin JM, Kim MY, Sohn KC, Jung SY, Lee HE, Lim JW, Kim S, Lee YH, Im M, Seo YJ, Kim CD, Lee JH, Lee Y, et al. Nrf2 negatively regulates melanogenesis by modulating PI3K/Akt signaling. *PLoS ONE*. 2014; 9: e96035.
50. Le Gal K, Ibrahim MX, Wiel C, Sayin VI, Akula MK, Karlsson C, Dalin MG, Akyurek LM, Lindahl P, Nilsson J, Bergo MO. Antioxidants can increase melanoma metastasis in mice. *Sci Transl Med*. 2015; 7:308re8.
51. Sanchez-Laorden B, Viros A, Girotti MR, Pedersen M, Saturno G, Zambon A, Niculescu-Duvaz D, Turajlic S, Hayes A, Gore M, Larkin J, Lorigan P, Cook M, et al. BRAF inhibitors induce metastasis in RAS mutant or inhibitor-resistant melanoma cells by reactivating MEK and ERK signaling. *Sci Signal*. 2014; 7: ra30.
52. Bravo-Cordero JJ, Magalhaes MA, Eddy RJ, Hodgson L, Condeelis J. Functions of cofilin in cell locomotion and invasion. *Nat Rev Mol Cell Biol*. 2013; 14:405–415.
53. Arber S, Barbayannis FA, Hanser H, Schneider C, Stanyon CA, Bernard O, Caroni P. Regulation of actin dynamics through phosphorylation of cofilin by LIM-kinase. *Nature*. 1998; 393:805–809.
54. Niwa R, Nagata-Ohashi K, Takeichi M, Mizuno K, Uemura T. Control of actin reorganization by Slingshot, a family of phosphatases that dephosphorylate ADF/cofilin. *Cell*. 2002; 108:233–246.
55. Kim JS, Huang TY, Bokoch GM. Reactive oxygen species regulate a slingshot-cofilin activation pathway. *Mol Biol Cell*. 2009; 20:2650–2660.
56. Tan M, Song X, Zhang G, Peng A, Li X, Li M, Liu Y, Wang C. Overexpression of adenylate cyclase-associated protein 1 is associated with metastasis of lung cancer. *Oncol Rep*. 2013; 30:1639–1644.
57. Li M, Yang X, Shi H, Ren H, Chen X, Zhang S, Zhu J, Zhang J. Downregulated Expression of the Cyclase-associated Protein 1 (CAP1) Reduces Migration in Esophageal Squamous Cell Carcinoma. *Jpn J Clin Oncol*. 2013; 43:856–864.
58. Ibanez IL, Policastro LL, Tropper I, Bracalente C, Palmieri MA, Rojas PA, Molinari BL, Duran H. H₂O₂ scavenging inhibits G1/S transition by increasing nuclear levels of p27KIP1. *Cancer Lett*. 2011; 305:58–68.
59. Rotblat B, Grunewald TG, Leprivier G, Melino G, Knight RA. Anti-oxidative stress response genes: bioinformatic analysis of their expression and relevance in multiple cancers. *Oncotarget*. 2013; 4:2577–2590. doi:10.18632/oncotarget.1658.
60. Bracalente C, Salguero N, Notcovich C, Müller CB, da Motta LL, Klamt F, Ibañez IL, Durán H. Reprogramming human A375 amelanotic melanoma cells by catalase overexpression: Reversion or promotion of malignancy by inducing melanogenesis or metastasis. *Oncotarget*. 2016; doi: 10.18632/oncotarget.9220.
61. Godic A, Poljsak B, Adamic M, Dahmane R. The role of antioxidants in skin cancer prevention and treatment. *Oxid Med Cell Longev*. 2014; 2014:860479.
62. Goodman M, Bostick RM, Kucuk O, Jones DP. Clinical trials of antioxidants as cancer prevention agents: past, present, and future. *Free Radic Biol Med*. 2011; 51: 1068–1084.
63. Sayin VI, Ibrahim MX, Larsson E, Nilsson JA, Lindahl P, Bergo MO. Antioxidants accelerate lung cancer progression in mice. *Sci Transl Med*. 2014; 6:221ra15.
64. Tarpey MM, Wink DA, Grisham MB. Methods for detection of reactive metabolites of oxygen and nitrogen: *in vitro* and *in vivo* considerations. *Am J Physiol Regul Integr Comp Physiol*. 2004; 286: R431–444.
65. Mukhopadhyay P, Rajesh M, Hasko G, Hawkins BJ, Madesh M, Pacher P. Simultaneous detection of apoptosis and mitochondrial superoxide production in live cells by flow cytometry and confocal microscopy. *Nat Protoc*. 2007; 2:2295–2301.
66. Mannervik B. Glutathione peroxidase. *Methods Enzymol*. 1985; 113:490–495.
67. Wendel A. Glutathione peroxidase. *Methods Enzymol*. 1981; 77:325–333.
68. Liu Y, Peterson DA, Kimura H, Schubert D. Mechanism of cellular 3-(4, 5-dimethylthiazol-2-yl)-2, 5-diphenyltetrazolium bromide (MTT) reduction. *J Neurochem*. 1997; 69:581–593.
69. Chen X, Zhang B, Yuan X, Yang F, Liu J, Zhao H, Liu L, Wang Y, Wang Z, Zheng Q. Isoliquiritigenin-induced differentiation in mouse melanoma B16F0 cell line. *Oxid Med Cell Longev*. 2012; 2012:534934.
70. Pezzoni M, Pizarro RA, Costa CS. Protective role of extracellular catalase (KatA) against UVA radiation in *Pseudomonas aeruginosa* biofilms. *J Photochem Photobiol B*. 2014; 131:53–64.